ACTA ABP BIOCHIMICA POLONICA

Vol. 64, No 3/2017
445–449
https://doi.org/10.18388/abp.2017_1593

Communication

Invasive Cx43^{high} sub-line of human prostate DU145 cells displays increased nanomechanical deformability*

Katarzyna Piwowarczyk[1#], Michał Sarna[2,3#], Damian Ryszawy[1] and Jarosław Czyż[1✉]

[1]Department of Cell Biology, Faculty of Biochemistry, Biophysics and Biotechnology, Jagiellonian University, Kraków, Poland; [2]Department of Biophysics, Faculty of Biochemistry, Biophysics and Biotechnology, Jagiellonian University, Kraków, Poland; [3]Department of Medical Physics and Biophysics, Faculty of Physics and Applied Computer Science, AGH University of Science and Technology, Kraków, Poland

Connexin(Cx)43^{high} cells are preferentially recruited to the invasive front of prostate cancer *in vitro* and *in vivo*. To address the involvement of Cx43 in the regulation of human prostate cancer DU145 cell invasiveness, we have analysed the nanoelasticity of invasive Cx43^{high} sub-sets of DU145 cells by atomic force microscopy (AFM). The Cx43^{high} DU145 cells displayed considerably higher susceptibility to mechanical distortions than the wild type DU145 cells. Transient Cx43 silencing had no effect on their elastic properties. Our data confirm the relationship between the invasive potential, Cx43 expression and nanoelasticity of the DU145 cells. However, they also show that Cx43 is not directly involved in the maintenance of DU145 invasive phenotype.

Key words: prostate cancer invasion, Cx43, cell elasticity, motility, AFM

Received: 18 March, 2017; revised: 18 April, 2017; accepted: 19 April, 2017; available on-line: 24 June, 2017

✉e-mail: jarek.czyz@uj.edu.pl
#These authors contributed equally to this work
*Preliminary report on this subject has been presented at the XLIV Winter School of the Faculty of Biochemistry, Biophysics and Biotechnology, Jagiellonian University, Zakopane, 2017.
Abbreviations: AFM, atomic force microscope; DMEM, Dulbecco's-modified Eagle medium; EMT, epithelial-mesenchymal transition; FBS, fetal bovine serum; GJIC, gap junctional intercellular communication; IgG, immunoglobulin G; kPa, kilopascals; PBS, phosphate-buffered saline; SDS, sodium dodecyl sulfate; S.E.M., standard error of the mean

INTRODUCTION

Metastatic cascade of prostate cancer is initiated by the expansion of invasive cell sub-populations(s) within a phenotypically heterogeneous tumour cell mass (Shibata & Shen, 2013; Sottoriva *et al*., 2010). These cells show the predilection to colonise distant organs, which results from their relatively high motility, susceptibility to chemotactic, haptotactic, parabaric and juxtacrinic signals (Miekus *et al*., 2005; Gupta & Massague, 2006; Langley & Fidler, 2007; Blick *et al*., 2008; Friedl & Wolf, 2010), and from their increased nanoelasticity (Kumar & Weaver, 2009; Suresh, 2007). Phenotypic switches regulating the recruitment of cancer cells to the "invasive front" of prostate tumour are determined by extrinsic "paracrine" and "parabaric" signals, and by the "by-stander" effects mediated by connexin-formed gap junctions (Mol *et al*., 2007; Czyz *et al*., 2012). However, the links between the function of connexins and the invasive potential of prostate cancer cells represent a still weakly explored aspect of prostate cancer progression.

The primary function of connexins is the formation of membrane channels that link cytoplasmatic compartments of neighbouring cells. They mediate the intercellular exchange of small molecules (<1.5 kDa; gap junctional intercellular coupling; GJIC), thus determining the tissue homeostasis (Maeda & Tsukihara, 2011). However, connexins are also involved in the cancer development (Naus & Laird, 2010). Whereas down-regulation of connexin expression is usually seen in primary tumours (Leithe *et al*., 2006), high Cx43 levels were found in the cells that constitute the "invasive front" of numerous cancers (Ito *et al*., 2000; Zhang *et al*., 2003; Pollmann *et al*., 2005; Kanczuga-Koda *et al*., 2006; Ryszawy *et al*., 2014). We have recently suggested a stage-dependent role for connexin(Cx)43 in the prostate cancer promotion and progression (Czyz, 2008; Czyz *et al*., 2012). For instance, the micro-evolution of highly deformable prostate cancer AT-2 sub-populations is promoted by a GJIC-independent cooperative Snail-1/Cx43 signalling (Ryszawy *et al*., 2014). Cx43 function in human DU145 prostate cancer cell invasiveness can also rely on its involvement in GJIC between cancer and endothelial cells (Piwowarczyk *et al*., 2014). On the other hand, the interrelations between Cx43 and the susceptibility of DU145 cells to mechanical distortions (i.e. their sensitivity to adverse mechanical stress during invasion) remained unaddressed. Here, we focused on the heterogeneity of nanomechanical DU145 cell properties and on the role of Cx43 in regulation of the DU145 cell elasticity.

MATERIALS AND METHODS

DU145 cell culture and transmigration. Human prostate carcinoma DU145 cells were cultivated in DMEM-F12 HAM medium supplemented with 10% FBS and antibiotics (all from Sigma, St. Louis, MO). In order to establish the invasive DU145 cell sub-sets, microporous membranes in a Boyden chamber were used (Corning; pore diameter – 8 μm; membrane diameter – 6.5 mm). Native DU145 cells were seeded at the density of 300 cells per mm^2 onto the membrane and allowed to transmigrate for 48 hours. Afterwards, the chambers were placed into another well and the progeny of DU145 cells that precipitated onto the original well bottom was propagated (giving rise to DU145_48 subset). The "second wave" of transmigrating DU145 cells was collected in the next well for 24 hours and their progeny was propagated (DU145_72 subset). Before further analyses, the DU145 sub-sets were cultivated for at least 15 generation times (5 passages at 1:8) (Szpak *et al.,* 2011).

Atomic force microscopy. For AFM analysis, cells were seeded onto Petri dishes at a density of 1000 cells/cm^2 and incubated overnight in DMEM supplemented with 10% FBS, at 37°C in a 5% CO_2 humidified atmo-

sphere. Nanomechanical studies were performed using the Agilent 5500 atomic force microscope (AFM, Agilent Technologies, Austin, Texas, USA), equipped with a temperature/CO_2 chamber. Measurements were carried out in a fresh PBS containing Mg^{2+} and Ca^{2+} ions and glucose (1 mg/ml) at 37°C. Optical preview was used during the measurements to ensure that the analyses were performed on cells displaying a typical morphology. Mechanical analysis was performed in a force spectroscopy mode (Dufrene, 2003). Force measurements were collected using 2 types of standard silicon nitride cantilevers (Veeco Probes, USA) with a nominal tip radius of <50 nm and of 20 nm, respectively. Spring constant calibration of the probes was made before and after mechanical analysis of cells using the thermal tune procedure. Before each cell was measured, its topography was imaged using a tapping mode to precisely localize the central region of a cell. To prevent any cell damage and to reduce any substrate-induced effects, the measurements were collected in the force ranges resulting in shallow indentations of the cells (<500 nm). The half opening angle of the AFM tip was 25°, and the Poisson ratio of the cell was taken to be 0.5, which is typical for soft biological materials (Touhami *et al.*, 2003). Curves from 10 to 20 randomly selected points were collected from the central region of the cell at a rate of 1 Hz. 10 force curves were measured at each point for statistical analysis. A total number of at least 20 cells was investigated for each DU145 cell population. The values of the Young's modulus were estimated from the force curves by converting force-displacement curves into force-indentation curves and fitting them with the modified Hertz model (Radmacher *et al.*, 1996). Young's modulus data were expressed as means ±SEM. Statistical analysis was performed using two-sample independent Student's *t*-test; *p≤0.05.

Immunocytochemistry and immunoblotting. For immunocytochemical visualization of Cx43, cells were fixed with methanol:acetone (7:3, –20°C), labeled with rabbit anti-Cx43 IgG (Sigma), Alexa Fluor® 488-conjugated goat anti-rabbit IgG (Invitrogen, Carlsbad, CA) and counterstained by 0.5 μg/ml bis-benzimide (Hoechst) (Baran *et al.*, 2009). Visualization of Cx43-positive plaques was performed with a Leica DMIRE2 microscope. For Western blot analyses, the DU145 cell cultures were dissolved in lysis buffer and cellular proteins were applied to 15% SDS-polyacrylamide gels, followed by their transfer to nitrocellulose membranes. Blots were exposed to primary rabbit polyclonal anti-Cx43 and mouse monoclonal anti-α-tubulin antibody (both from Sigma) followed by detection of the antibodies using HRP-labelled secondary antibodies (Invitrogen) and a SuperSignal West Pico Substrate (Pierce, Rockford, IL) (Daniel-Wojcik *et al.*, 2008).

siRNA inhibition of Cx43 expression. DU145 cells were seeded at a density of 7×10^4 cells per well in a 12-well plate in an antibiotic-free DMEM-F12 HAM medium supplemented with 10% FBS and grown overnight at 37°C. MISSION®esiRNA GJA1 (114 pmol, Sigma) and Lipofectamine™2000 (Invitrogen) were used for transient Cx43 silencing in the DU145_48 cells according to the manufacturer's protocol (Piwowarczyk *et al.*, 2015). The efficiency of the inhibition of Cx43 expression was subsequently analysed by using immunoblotting. Endpoint analyses were performed 48 hours after transfection.

RESULTS AND DISCUSSION

Invasive Cx43^{high} DU145 cells display relatively high deformability

We have previously described the heterogeneity of the basic DU145 traits crucial for their invasiveness, including the motility and Cx43 expression (Szpak *et al.*, 2011). The existence of invasive subpopulations within the DU145 cell line prompted us to perform single-cell analyses of long-term relationship between the Cx43

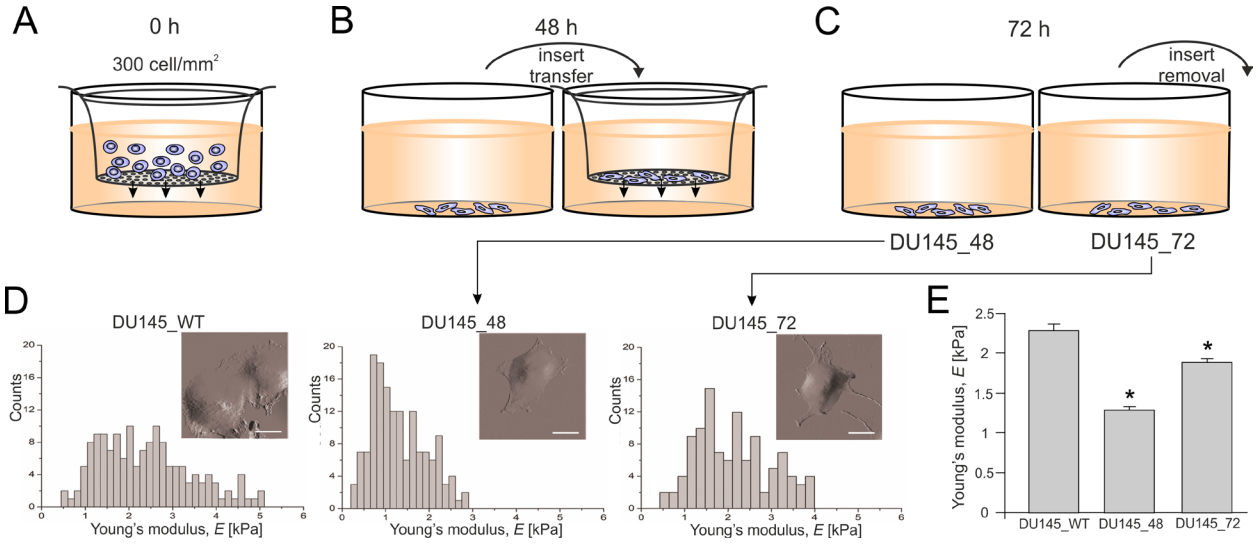

Figure 1. Efficiency of the DU145 cell transmigration correlates with a relatively high nanomechanical elasticity of the DU145 cells. (**A**) DU145 cells were seeded onto microporous membranes (pore diameter-8 μm) at the density of 300 cells per mm². The cells were allowed to transmigrate across the pores and the chambers were placed in another well 48 h thereafter (**B**). After the next 24 h, the inserts were moved to another well and allowed to transmigrate for 24 h (**C**). The cells in each well were propagated to obtain the DU145_48 and DU145_72 subset. (**D**) AFM analyses revealed a significantly increased fraction of deformable cells within the DU145_48 subset (middle) and a slight enrichment of the DU145_72 subset in deformable cells (right), when compared to the "wild type" DU145 cells (left). Pictures represent a scan size equal to 45×45 μm (scale bar – 5 μm). (**E**) The average values of Young's modulus estimated for each population and given in kilopascals (kPa). Results are representative of 3 independent experiments. *p<0.05 (two-sample independent Student's *t*-test).

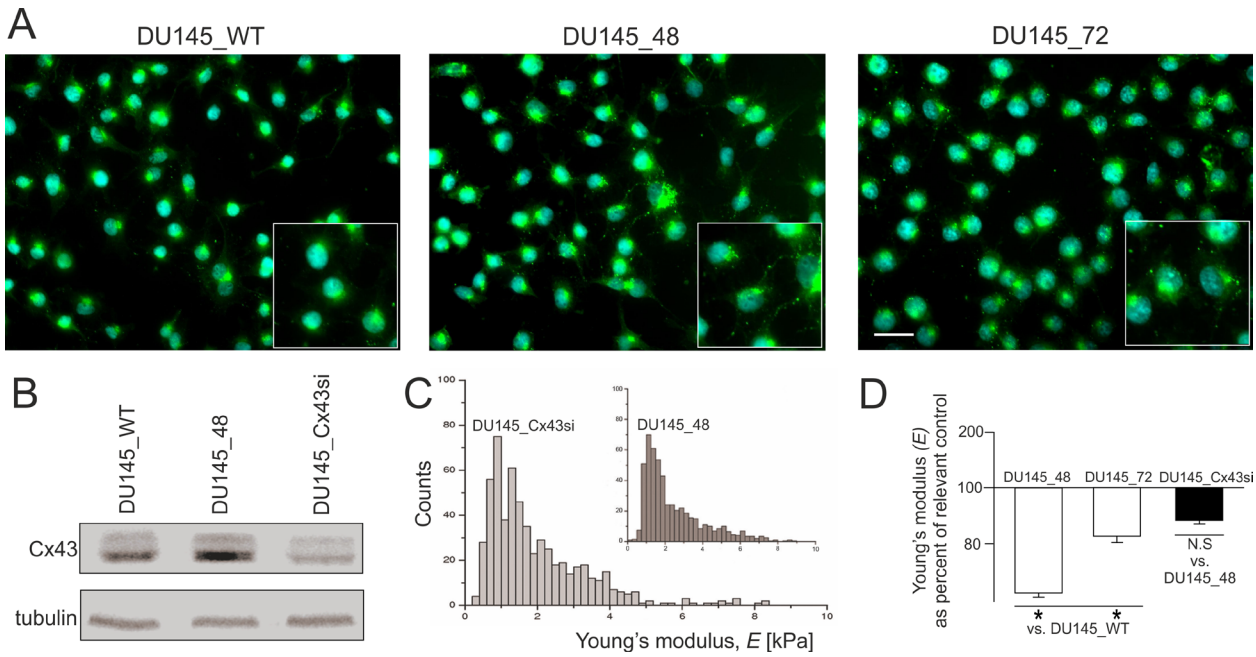

Figure 2. Cx43 silencing does not affect the nanomechanical elasticity of the DU145_48 cells.
(**A**) Cx43-positive plaques were more abundant in the DU145_48 and DU145_72 subset than in the wild type DU145 populations. Bar – 25 μm. Transient down-regulation of Cx43 in the DU145_48 cells (**B**) did not affect their elasticity (**C**). Values of E represent the Young's modulus given in kilopascals (kPa). (**D**) The average values of Young's modulus estimated for the DU145_48 and DU145_72 cells (in comparison to the DU145_WT cells; open bars) and of the DU145_48 cells after Cx43 silencing (DU145_Cx43si) compared to the control DU145_48 cells (filled bar). Results are representative of 3 independent experiments. Error bars represent S.E.M. *$p<0.05$ (two-sample independent Student's *t*-test).

function and the nanoelasticity of those cells. For this purpose, sub-lines of the DU145 cells were propagated from single cells that most readily transmigrated microporous membranes under isotropic conditions, i.e. in the absence of chemoattractant gradients (Fig. 1A). We have established two invasive sub-lines of the DU145 cells: the DU145_48 cells represented the progeny of a minute (ca. 2%) transmigrating cell population (Fig. 1B). The DU145_72 sub-set were propagated from the "second wave" of transmigrating DU145 cells (Fig. 1C). As shown previously, such DU145 subsets are characterised by similar motile activity (Szpak *et al*., 2011). Therefore, we further analysed elastic properties of both DU145 subsets with atomic force microscopy (AFM) to estimate the role of the susceptibility to mechanical distortions in regulation of the DU145 invasive potential.

Values of Young's modulus (E) estimated for individual "wild type" DU145 cells were almost equally distributed between 1.0 to 3.0 kPa (Fig. 1D). However, a considerable (roughly 25%) fraction of cells characterized by E>3 kPa could be also discriminated, whilst only a minute set of wild type DU145 cells displayed E=0.5–1.0 kPa. Importantly, the DU145_48 cell sub-line was considerably enriched in "elastic" cells characterized by E<1 kPa (30%). The fraction of cells displaying E values between 1.0 to 3.0 kPa (which were dominant in "native" DU145 populations) was less numerous in the DU145_48 sub-set. In these analyses, we did not observe the events of E>3 kPa. The cells that comprised the "second wave" of DU145 transmigration gave a progeny (DU145_72), which was characterised by E values distribution more similar to that observed for the wild type DU145 populations. It ranged between 0.5 to 4.2 kPa, with several local maxima (1.5 kPa, 2.4 kPa and 3.3 kPa). Moreover, some events of E>3 kPa (absent in the DU145_48 sub-line) were seen in the DU145_72 populations. The difference in the distribution of E values observed between the analyzed DU145 populations is also illustrated by the difference in the averaged values of Young's modulus (E) calculated for each population (Fig. 1E).

Invasive DU145 sub-sets were analysed between the 5th and 15th passage after transmigration. Therefore, these data show that single DU145 cells can give rise to progeny characterised by heritably increased deformability, which may potentially facilitate their invasion *in vivo*. They also confirm that microevolutionary processes that are responsible for the *in vivo* formation of prostate cancer invasive front may be recapitulated *in vitro*. Previously, no differences in the motile activity, morphology and the architecture of actin cytoskeleton were observed between DU145_48, DU145_72 and "native" DU145 cells (Szpak *et al*., 2011). Thus, the nanomechanical elasticity of the DU145 cells is a primary determinant of their transmigration potential (Friedl & Wolf, 2010; Kumar & Weaver, 2009). A similar interrelation between increased susceptibility to mechanical distortions and the invasiveness was observed in breast cancer cells (Li et al., 2008). Persistence of cellular invasive phenotype through multiple cell division cycles is mandatory for cancer invasion. Phenotypic persistence of the DU145 sub-sets demonstrates that the observed differences in cell elasticity result from permanent cell reprogramming rather than from "secular" changes of cell shape and adhesion (Gupta & Massague, 2006; Langley & Fidler, 2007; Friedl & Wolf, 2010; Ryszawy *et al*., 2014).

We have previously shown the involvement of Cx43 in regulation of the nanoelasticity of the rat prostate carcinoma AT-2 cells (Ryszawy *et al*., 2014). These cells reacted to ectopic Cx43 down-regulation with a considerable increase of their mechanical stiffness. Immunofluorescence and immunoblot analyses confirmed that the

DU145_48 population is characterized by elevated levels of Cx43 in comparison to the "native" DU145 and DU145_72 cells (Fig. 2A). This observation confirms that the nanoelasticity Cx4^{high} DU145 cells is somehow linked to the Cx43 function. To elucidate whether Cx43 directly participates in regulation of the nanomechanical properties of the DU145 cells, we transiently silenced Cx43 in the DU145_48 cells (Fig. 2B) and analysed their elasticity by AFM. For this purpose, we used more precise (20 nm tip) cantilevers to increase the resolution of the technique. Ectopic Cx43 down-regulation did not increase the mechanical stiffness of the DU145_48 cells (Fig. 2C; summarized in Fig. 2D). A similar distribution of E values was detected by AFM analyses of the control and Cx43siRNA-transfected DU145_48si cells. These data stay in agreement with our previous observations showing that Cx43 silencing and chemical inhibition of GJIC does not affect the relative abundance of Cx43^{high} DU145 cells in the invasive front (Szpak *et al*., 2011). However, they contradict the suggestions on the Cx43 regulatory role in the regulation of cancer cells' susceptibility to mechanical distortions (Cronier *et al*., 2009). Even though Cx43 has been implicated in the regulation of AT-2 cell elasticity (Ryszawy *et al*., 2014), apparently it is not involved in the determination of DU145 elasticity. Collectively, Cx43 may accompany the relatively high deformability of individual DU145 cells, which decreases their sensitivity to adverse mechanical stress factors during the invasion process. However, it is not directly involved in its regulation.

CONCLUSION

Microevolution of "invasive" cell subpopulations characterised by increased susceptibility to mechanical distortions is crucial for the "metastatic cascade" of numerous cancers (Cross *et al*., 2007; Gupta & Massague, 2006; Suresh, 2007; Cai *et al*., 2010). Cx43 is involved in the evolutionary processes which are crucial for metastatic cascade of prostate cancer (Watanabe *et al*., 2002; Miekus *et al*., 2005; Langley & Fidler, 2007; Blick *et al*., 2008). A selective transmigration of Cx43^{high} prostate cancer DU145 cell sub-populations under the conditions mimicking early cancer invasion confirmed our earlier reports on such microevolution in the prostate cancer cell populations *in vitro*. However, an apparently coincidental nature of the correlation between Cx43^{high} phenotype of the DU145 cells and their susceptibility to mechanical distortions remains in contrast to our previous observations on mechanistic involvement of Cx43 in the process of epithelial-mesenchymal transition (EMT) of the AT-2 cells (Ryszawy *et al*., 2014). These contrasting data show the complexity and tissue-specificity of the relationship between cell invasiveness, Cx43 expression and the nanomechanical elasticity of cancer cells, which govern the metastatic cascade of prostate cancer. They expand our knowledge on the subtlety of interactions between Cx43 and cytoskeleton (Prochnow & Dermietzel, 2008; Cronier *et al*., 2009; Olk *et a*l., 2009) in the regulation of cancer cell adhesion, directed motility, susceptibility to mechanical distortions and sensitivity to adverse mechanical stress during invasion (Suresh, 2007; Kumar & Weaver, 2009; Shibata & Shen, 2013). A more comprehensive study on Cx43 involvement in the regulation of the nanoelasticity of prostate cancer cells, performed on an array of prostate cancer cell lineages derived from biopsies, is necessary to fully understand the differences in the relationship between Cx43 levels and invasiveness, observed between the AT-2 and DU145 lineages. This should help to fully assess specificity and heterogeneity of Cx43 functions in the regulation of the metastatic potential of prostate cancer cells.

Conflicts of interest

The authors declare no conflict of interest.

Acknowledgements

The Faculty of Biochemistry, Biophysics and Biotechnology of the Jagiellonian University is a partner of the Leading National Research Center (KNOW) supported by the Ministry of Science and Higher Education.

Funding

This work was financially supported by the National Science Centre, Poland (grant 2015/17/B/NZ3/01040 to J. Czyż).

REFERENCES

Baran B, Bechyne I, Siedlar M, Szpak K, Mytar B, Sroka J, Laczna E, Madeja Z, Zembala M, Czyz J (2009) Blood monocytes stimulate migration of human pancreatic carcinoma cells in vitro: the role of tumour necrosis factor – alpha. *Eur J Cell Biol* **88**: 743–752. doi: 10.1016/j.ejcb.2009.08.002

Blick T, Widodo E, Hugo H, Waltham M, Lenburg ME, Neve RM, Thompson EW (2008) Epithelial mesenchymal transition traits in human breast cancer cell lines. *Clin Exp Metastasis* **25**: 629–642. doi: 10.1007/s10585-008-9170-6

Cai X, Xing X, Cai J, Chen Q, Wu S, Huang F (2010) Connection between biomechanics and cytoskeleton structure of lymphocyte and Jurkat cells: An AFM study. *Micron* **41**: 257–262. doi: 10.1016/j.micron.2009.08.011

Cronier L, Crespin S, Strale PO, Defamie N, Mesnil M (2009) Gap junctions and cancer: new functions for an old story. *Antioxid Redox Signal* **11**: 323–338. doi: 10.1089/ars.2008.2153

Cross SE, Jin YS, Rao J, Gimzewski JK (2007) Nanomechanical analysis of cells from cancer patients. *Nat Nanotechnol* **2**: 780–783. doi: 10.1038/nnano.2007.388

Czyz J (2008) The stage-specific function of gap junctions during tumourigenesis. *Cell Mol Biol Lett* **13**: 92–102. doi: 10.2478/s11658-007-0039-5

Czyz J, Szpak K, Madeja Z (2012) The role of connexins in prostate cancer promotion and progression. *Nat Rev Urol* **9**: 274–282. doi: 10.1038/nrurol.2012.14

Daniel-Wojcik A, Misztal K, Bechyne I, Sroka J, Miekus K, Madeja Z, Czyz J (2008) Cell motility affects the intensity of gap junctional coupling in prostate carcinoma and melanoma cell populations. *Int J Oncol* **33**: 309–315. doi: 10.3892/ijo_00000010

Dufrene YF (2003) Recent progress in the application of atomic force microscopy imaging and force spectroscopy to microbiology. *Curr Opin Microbiol* **6**: 317–323. doi: 10.1016/S1369-5274(03)00058-4

Friedl P, Wolf K (2010) Plasticity of cell migration: a multiscale tuning model. *J Exp Med* **207**: 11–19. doi: 10.1083/jcb.200909003

Gupta GP, Massague J (2006) Cancer metastasis: building a framework. *Cell* **127**: 679–695. doi: 10.1016/j.cell.2006.11.001

Ito A, Katoh F, Kataoka TR, Okada M, Tsubota N, Asada H, Yoshikawa K, Maeda S, Kitamura Y, Yamasaki H, Nojima H (2000) A role for heterologous gap junctions between melanoma and endothelial cells in metastasis. *J Clin Invest* **105**: 1189–1197. doi: 10.1172/JCI8257

Kanczuga-Koda L, Sulkowski S, Lenczewski A, Koda M, Wincewicz A, Baltaziak M, Sulkowska M (2006) Increased expression of connexins 26 and 43 in lymph node metastases of breast cancer. *J Clin Pathol* **59**: 429–433. doi: 10.1136/jcp.2005.029272

Kumar S, Weaver VM (2009) Mechanics, malignancy, and metastasis: the force journey of a tumor cell. *Cancer Metastasis Rev* **28**: 113–127. doi: 10.1007/s10555-008-9173-4

Langley RR and Fidler IJ (2007) Tumor cell-organ microenvironment interactions in the pathogenesis of cancer metastasis. *Endocr Rev* **28**:297-321; doi: 10.1210/er.2006-0027

Leithe E, Sirnes S, Omori Y, Rivedal E (2006) Downregulation of gap junctions in cancer cells. *Crit Rev Oncog* **12**: 225–256. doi: 10.1615/CritRevOncog.v12.i3-4.30

Li QS, Lee GY, Ong CN, Lim CT (2008) AFM indentation study of breast cancer cells. *Biochem Biophys Res Commun* **374**: 609–613. doi: 10.1016/j.bbrc.2008.07.078

Maeda S, Tsukihara T (2011) Structure of the gap junction channel and its implications for its biological functions. *Cell Mol Life Sci* **68**: 1115–1129. doi: 10.1007/s00018-010-0551-z

Miekus K, Czernik M, Sroka J, Czyz J, Madeja Z (2005) Contact stimulation of prostate cancer cell migration: the role of gap junctional coupling and migration stimulated by heterotypic cell-to-cell contacts in determination of the metastatic phenotype of Dunning rat prostate cancer cells. *Biol Cell* **97**: 893–903. doi: 10.1042/BC20040129

Mol AJ, Geldof AA, Meijer GA, van der Poel HG, van Moorselaar RJ (2007) New experimental markers for early detection of high-risk prostate cancer: role of cell-cell adhesion and cell migration. *J Cancer Res Clin Oncol* **133**: 687–695. doi: 10.1007/s00432-007-0235-8

Naus CC, Laird DW (2010) Implications and challenges of connexin connections to cancer. *Nat Rev Cancer* **10**: 435–441. doi: 10.1038/nrc2841

Olk S, Zoidl G, Dermietzel R (2009) Connexins, cell motility, and the cytoskeleton. *Cell Motil Cytoskeleton* **66**: 1000–1016. doi: 10.1002/cm.20404

Piwowarczyk K, Wybieralska E, Baran J, Borowczyk J, Rybak P, Kosinska M, Wlodarczyk AJ, Michalik M, Siedlar M, Madeja Z, Dobrucki J, Reiss K, Czyz J (2015) Fenofibrate enhances barrier function of endothelial continuum within the metastatic niche of prostate cancer cells. *Expert Opin Ther Targets* **19**: 163–176. doi: 10.1517/14728222.2014.981153

Pollmann MA, Shao Q, Laird DW, Sandig M (2005) Connexin 43 mediated gap junctional communication enhances breast tumor cell diapedesis in culture. *Breast Cancer Res* **7**: R522–R534. doi: 10.1186/bcr1042

Prochnow N, Dermietzel R (2008) Connexons and cell adhesion: a romantic phase. *Histochem Cell Biol* **130**: 71–77. doi: 10.1007/s00418-008-0434-7

Radmacher M, Fritz M, Kacher CM, Cleveland JP, Hansma PK (1996) Measuring the viscoelastic properties of human platelets with the atomic force microscope. *Biophys J* **70**: 556–567. doi: 10.1016/S0006-3495(96)79602-9

Ryszawy D, Sarna M, Rak M, Szpak K, Kedracka-Krok S, Michalik M, Siedlar M, Zuba-Surma E, Burda K, Korohoda W, Madeja Z, Czyz J (2014) Functional links between Snail-1 and Cx43 account for the recruitment of Cx43-positive cells into the invasive front of prostate cancer. *Carcinogenesis* **35**: 1920–1930. doi: 10.1093/carcin/bgu033

Shibata M, Shen MM (2013) The roots of cancer: Stem cells and the basis for tumor heterogeneity. *Bioessays* **35**: 253–260. doi: 10.1002/bies.201200101

Sottoriva A, Verhoeff JJ, Borovski T, McWeeney SK, Naumov L, Medema JP, Sloot PM, Vermeulen L (2010) Cancer stem cell tumor model reveals invasive morphology and increased phenotypical heterogeneity. *Cancer Res* **70**: 46–56. doi: 10.1158/0008-5472.CAN-09-3663

Suresh S (2007) Biomechanics and biophysics of cancer cells. *Acta Biomater* **3**: 413–438. doi: 10.1016/j.actbio.2007.04.002

Szpak K, Wybieralska E, Niedzialkowska E, Rak M, Bechyne I, Michalik M, Madeja Z, Czyz J (2011) DU-145 prostate carcinoma cells that selectively transmigrate narrow obstacles express elevated levels of CX43. *Cell Mol Biol Lett* **16**: 625–637. doi: 10.2478/s11658-011-0027-7

Touhami A, Nysten B, Dufrene YF (2003) Nanoscale mapping of the elasticity of microbial cells by atomic force microscopy. *Langmuir* **19**: 4539–4543. doi: 10.1021/la034136x

Watanabe N, Dickinson DA, Krzywanski DM, Iles KE, Zhang H, Venglarik CJ, Forman HJ (2002) A549 subclones demonstrate heterogeneity in toxicological sensitivity and antioxidant profile. *Am J Physiol Lung Cell Mol Physiol* **283**: L726–L736. doi: 10.1152/ajplung.00025.2002

Zhang W, DeMattia JA, Song H, Couldwell WT (2003) Communication between malignant glioma cells and vascular endothelial cells through gap junctions. *J Neurosurg* **98**: 846–853. doi: 10.3171/jns.2003.98.4.0846